Photoelectrochemical properties of dye-dispersing allophane–titania composite electrodes

Hiromasa Nishikiori [1,*], Naohiro Kanada [1], Rudi Agus Setiawan [1], Koji Morita [1], Katsuya Teshima [1], Tsuneo Fujii [2]

[1]Department of Environmental Science and Technology, Faculty of Engineering, Shinshu University, 4-17-1 Wakasato, Nagano 380-8553, Japan

[2]Nagano Prefectural Institute of Technology, 813-8 Shimonogo, Ueda, Nagano 386-1211, Japan

Corresponding author: Hiromasa Nishikiori

Tel: +81-26-269-5536

Fax: +81-26-269-5531

E-mail: nishiki@shinshu-u.ac.jp

Department of Environmental Science and Technology, Faculty of Engineering, Shinshu University, 4-17-1 Wakasato, Nagano 380-8553, Japan

Abstract

Dye-dispersing allophane–titania composite electrodes were prepared from titanium alkoxide sols containing dye and allophane. The photoelectric conversion properties of the electrodes were investigated by photoelectrochemical measurements. The photocurrent values in the UV range decreased with an increase in the allophane content, whereas those in the visible range were increased by adding 1.0% (Al/Ti ratio) allophane. As a small amount of allophane nanoparticles were highly dispersed in the titania electrodes, the dye molecules were dispersed in the electrodes without decreasing the efficiency of the electron injection from the dye to the titania conduction band. The dye molecules dispersed on the titania nanoparticle surface were capped with allophane nanoparticles which prevented desorption. The dye molecules strongly interacted with the titania nanoparticle surface and efficiently injected the excited electrons into the titania conduction band.

Keywords: allophane; titania; fluorescein; photoelectrochemistry; electron injection

1. Introduction

Adsorption is important for a photocatalytic reaction process involving direct oxidation and reduction by the photogenerated holes and electrons. Natural clay minerals have attracted considerable attention as unique and functional adsorbents (Bergaya et al., 2006; Cea et al., 2007; Xu et al., 1998). The clay–titania composites were studied for the effective adsorption and degradation of organic compounds (Hewer et al., 2009; Kitayama et al., 1998; Suárez et al., 2008; Tao et al., 1999; Yoneyama et al., 1989). Allophane, a natural clay mineral distributed throughout the world, is a hydrated aluminosilicate ($1–2SiO_2•Al_2O_3•5–6H_2O$) having a 3.5–5.0 nm-sized hollow spherical structure with 0.3–0.5 nm-sized defects on its surface (Hall et al., 1985; Henmi and Wada, 1976; Kitagawa, 1971; van der Gaast et al., 1985; Wada and Wada, 1977). The walls of the hollow spheres consist of inner silica and outer alumina layers with a hydroxylated or hydrated surface. Some studies suggest that these surfaces have a significant ability to adsorb ionic or polar pollutants due to their amphoteric ion-exchange activity and high surface area (Hall et al., 1985; Kitagawa, 1971; Hanudin et al., 1999). Allophane consists of the smallest structural units of all the clay minerals. The clay–titania composites can be effective in degrading organic compounds if the adsorbed molecules are quickly brought to the titania surface. However, hybridization of the clay minerals with the photocatalysts decreased their photocatalytic activity because such clay minerals consist of relatively large-sized insulative particles. There is a

possibility that the high dispersion of allophane nanoparticles on the photocatalyst surface allows retention of the semiconductivity and activity.

In our previous study, a highly adsorptive allophane–titania nanocomposite photocatalyst was prepared by dispersing allophane nanoparticles into the titania by the sol-gel method (Nishikiori et al, 2011a). During the photocatalytic degradation of trichloroethylene using the allophane–titania nanocomposite, emission of the intermediate product, phosgene, was drastically inhibited. These compounds were rapidly adsorbed on the allophane, then gradually degraded after diffusing to the titania.

The electronic application of photocatalysts is being developed in various fields such as photovoltaic cells due to their semiconducting properties. Photocatalyst titania films are widely studied as dye-sensitized solar cell electrodes and are approaching their practical use (Grätzel, 2003). They are also useful as photofuel cell electrodes to generate electricity assisted by oxidizing the fuel materials during UV irradiation (Antoniadou and Lianos, 2010; Antoniadouet al., 2010; Kaneko et al., 2006; Ueno et al., 2009). The organic compounds added to the electrolyte solutions prevent the backward processes due to efficient consumption of the electrons and holes. In such systems, the concentration of the fuel material on the photocatalyst surface is one of the variables for improving the energy conversion efficiency (Nishikiori et al., 2011b, 2012a). A method to increase the concentration is the use of the appropriate adsorbents. Actually, a higher short circuit current was observed in a photofuel cell using the 0.10% allophane-containing titania electrode than

that with the normal titania electrode (Nishikiori et al., 2012b, 2014a). Allophane effectively adsorbed the glucose and starch molecules and then brought them close to the titania nanoparticles, on which their oxidation induced the electrogeneration.

The sol–gel reaction using a titanium alkoxide sol containing the dye molecules without heating easily allows the formation of the dye-dispersing titania films, which are amorphous or nanocrystalline (Brinker and Scherer, 1990; Brinker et al., 1991a, 1991b; Dislich, 1971a, 1983). In such systems, the dye molecules can be highly dispersed on the surface of the individual titania nanoparticles without their aggregation. The dye–titania electronic interaction is very important for the electron injection process in the photovoltaic materials such as the dye-sensitized solar cells (El Mekkawi and Abdel-Mottaleb, 2005; Grätzel, 2003; Sharma et al., 2009). The functional groups were induced in the sensitized dye molecules in order to form a strong bond between the dye chromophore and the titania surface (El Mekkawi and Abdel-Mottaleb, 2005; Hilgendorff and Sundström, 1998; Ramakrishna and Ghosh, 2001). Each molecule prefers to be strongly bonded to the titania surface for an efficient electron injection and reducing the energy transfer between the molecules which form the aggregates.

In such systems, a significant number of dye molecules prefer to be highly dispersed on the individual titania nanoparticles. Allophane is expected to increase the number of dye molecules due to its high adsorption ability. In this study, the dye-dispersing allophane–titania composite electrodes were prepared from titanium alkoxide sols containing the dye and allophane. A

fluorescein dye, which has been used in our systematic study of dye-dispersing titania electrodes, was used as a sensitizer. The dye–titania interaction and photoinduced electron transfer can be evaluated by photocurrent measurements as previously reported (Nishikiori et al., 2011c, 2012c, 2014b; Setiawan et al., 2013). The spectroscopic and photoelectric conversion properties of the dye-dispersing allophane–titania composite electrodes were investigated in order to clarify the influences of the dye and allophane dispersion on the electron transfer properties.

2. Experimental

2.1. Materials

Fluorescein, ethanol, titanium tetraisopropoxide, nitric acid, hydrochloric acid, diethylene glycol, iodine, and lithium iodide (Wako, S or reagent grade) were used without further purification. The water was deionized and distilled. Glass plates coated with the indium tin oxide (ITO) transparent electrode (60 mm × 25 mm) (AGC Fabritec) were soaked in hydrochloric acid (1.0 mol dm^{-3}) for 1 h, then rinsed with water. The electrolyte for the photoelectric measurement consisted of a diethylene glycol solution of iodine (5.0×10^{-2} mol dm^{-3}) and lithium iodide (0.50 mol dm^{-3}). The allophane ($1.6SiO_2{\cdot}Al_2O_3{\cdot}5–6H_2O$) was extracted by elutriation of Kanuma soil from Tochigi, Japan, as previously described (Nishikiori et al., 2009, 2010).

2.2. Sample preparation

The sol–gel reaction system was prepared by mixing 5.0 cm^3 of titanium tetraisopropoxide, 25.0 cm^3 of ethanol, 0.21 cm^3 of water, and 0.21 cm^3 of concentrated nitric acid as the catalyst for the sol–gel reaction and labeled S0. The concentration of nitric acid was 7.5×10^{-2} mol dm^{-3} in the S0. Fluorescein was dissolved in the S0 at a concentration of 1.0×10^{-2} mol dm^{-3}, which was labeled S0-f. The allophane was dispersed in the S0 and S0-f in which the Al/(Al+Ti) ratios were 0 (0% allophane), 1/1000 (0.10% allophane), 1/100 (1.0% allophane), and 1/10 (10% allophane). The sol–gel systems with and without fluorescein and/or allophane were agitated and allowed to react during ultrasonication for 1 day. The glass plates with the ITO transparent electrode were dip-coated 3 times with the S0 and then heated at 500ºC for 30 min in order to prepare the anatase-type titania electrodes. This layer plays the role as a blocking layer in order to suppress the charge recombination at the interface between the upper layer and the ITO layer (Cameron and Peter, 2003; Hart et al., 2006; Patrocinio et al., 2009). These electrodes were dip-coated 5 times with the S0 containing 0%, 0.10%, 1.0%, and 10% allophane and then steam-treated at 100°C for 120 min. The dye-free electrodes were immersed in fluorescein ethanol solution at a concentration of 1.0×10^{-3} mol dm^{-3} for 24 h in order to prepare the dye-adsorbing allophane–titania composite electrodes. On the other hand, the titania-based electrodes were dip-coated 5 times with the S0-f containing 0%, 0.10%, 1.0%, and 10% allophanes and then steam-treated at 100°C for 120 min in order to prepare the dye-dispersing allophane–titania composite electrodes. The glass plates without the ITO were also coated with the sols in order to measure the XRD patterns.

2.3. Measurements

The surface morphology of the electrode samples was observed, and their layer thickness was estimated from their cross section using a field emission scanning electron microscope (Hitachi S-4100). The crystalline phase was determined using an X-ray diffractometer (Rigaku RINT-2200V). The flakes of the film and powder samples were pressed in KBr pellets and their IR spectra were obtained using an FTIR spectrophotometer (Shimadzu FTIR-8300).

The iodine-based electrolyte was allowed to soak into the space between the electrode sample and the Pt counter-electrode. Monochromatic light from a fluorescence spectrophotometer (Shimazdu RF-5300) with a 150 W Xe short arc lamp (Ushio UXL-155) was irradiated on the electrodes for the spectroscopic measurements. During the light irradiation, the short circuit currents of the electrodes were measured in the electrolyte solutions by a digital multimeter (ADCMT 7461A). The *J–V* curves of the electrodes were measured by a potentiostat (Hokuto Denko HSV-100) during the visible light (0.40 W cm^{-2}) irradiation at a wavelength longer than 400 nm emitted by the 150 W Xe short arc lamp using a sharp cutoff filter. The intensity at each wavelength of the light source was obtained using a power meter (Molectron PM500A) in order to estimate the incident photon-to-current conversion efficiency (IPCE) and quantum efficiency for the photocurrent from the excited ligands, i.e., absorbed photon-to-current quantum efficiency (APCE), in the electrode samples. The visible absorbance of the present electrode samples was lower than 1.0 which was sufficient to measure the number of absorbed photons in order to calculate the quantum efficiency.

3. Results and discussion

3.1. Characterization of the electrodes

Figure 1 shows the SEM images of the surface of the dye-dispersing titania and allophane–titania composite electrodes. The films consist of 10–30-nm-sized particles regardless of the allophane content and cannot be distinguished because the allophane particles are very small (Nishikiori et al., 2011a). The thickness of the titania layer was ca. 400 nm as previously reported. The TEM image of the 1.0% allophane–titania composite powder was previously reported (Nishikiori et al., 2012b, 2014a). The allophane consisted of ca. 5-nm-sized porous particles. In the image of the composite, the ca. 10-nm-sized particles, which exhibited lattice fringes, should indicate the titania particles. Many small amorphous particles of allophane were dispersed on the titania particle surface. The allophane particles were tightly attached to the titania surface.

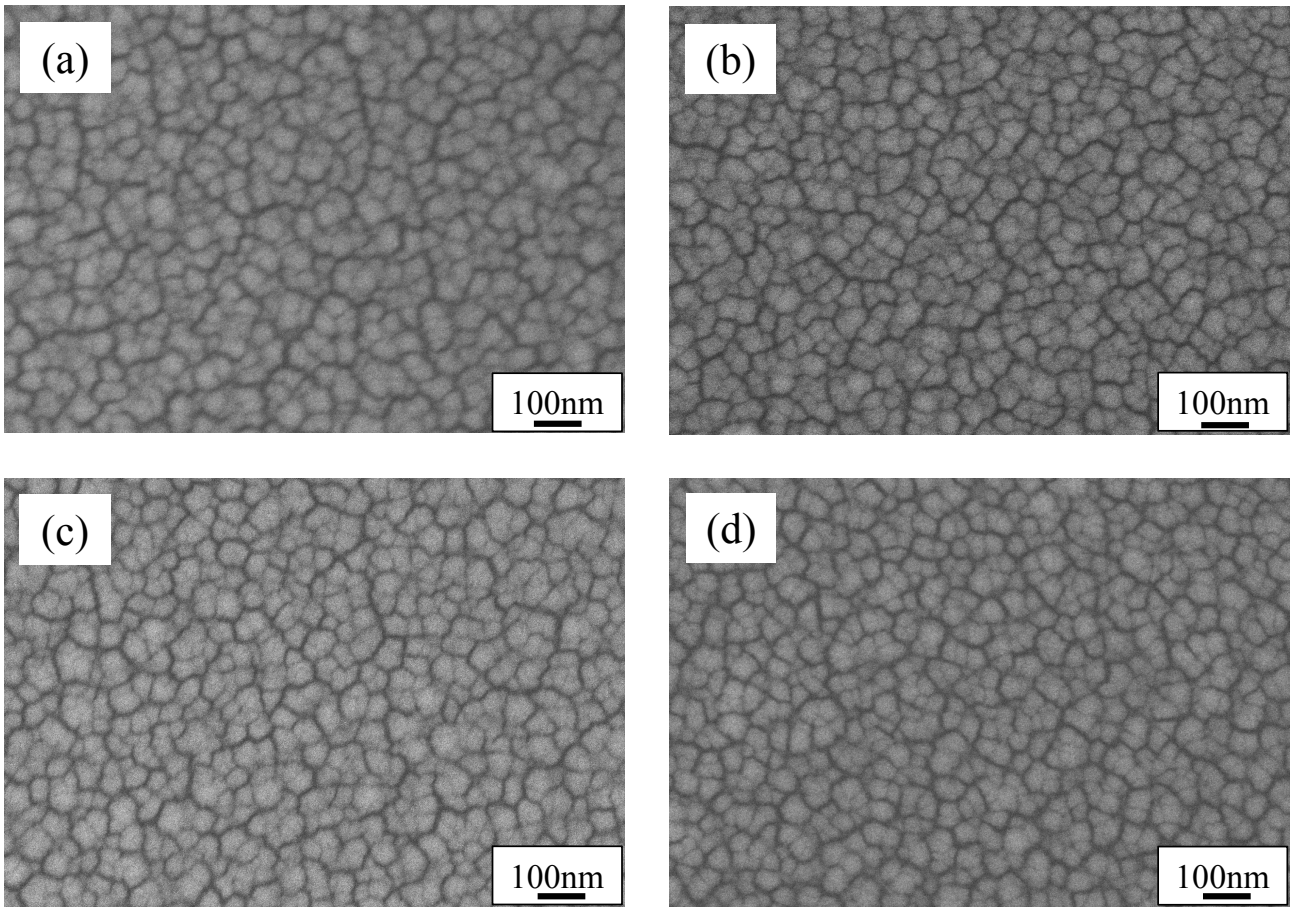

Figure 1 SEM images of the (a) dye-dispersing titania, (b) 0.10% allophane–titania composite, (c) 1.0% allophane–titania composite, and (d) 10% allophane–titania composite electrodes.

Figure 2 shows the XRD patterns of the dye-dispersing titania and allophane–titania composite films. The peaks at around 25.3º, 37.8º, and 48.1 º are assigned to the (101), (004), and (200) planes of the anatase-type titania in all the films, respectively. Their crystallite size was estimated from the full-width at half-maximum of the 25.3° peak using Sherrer's equation to be 8.2 nm for the titania, 8.1 nm for the 0.10% allophane–titania composite, 6.2 nm for the 1.0% allophane–titania composite, and 4.5 nm for the 10% allophane–titania composite. The sizes were smaller for the allophane-containing films than for only the titania film. This result indicated that the allophane

particles prevented the crystal growth of the titania because they were highly dispersed in the entire film and strongly bonded to the titanium alkoxide polymers and the titania gel particles (Nishikiori et al., 2011a, 2012b, 1014a). The dispersion of allophane particles influenced the particle growth and crystallization process of the titania.

In previous studies, no peak was observed for the ligand-dispersing films, indicating that the strong interaction between the titanium species of the titania precursor and the ligand molecules significantly suppressed the crystal growth during the steam treatment (Kitsui et al., 2006; Nishikiori et al., 2013a). These results can be interpreted as the ligand molecules preventing crystallization of the gel around them. On the other hand, the titania crystallite size of the fluorescein-dispersing titania films did not depend on the dye concentration. The crystal growth of the titania depended on the interaction between the dye molecules and titania in the dye-dispersing titania systems.

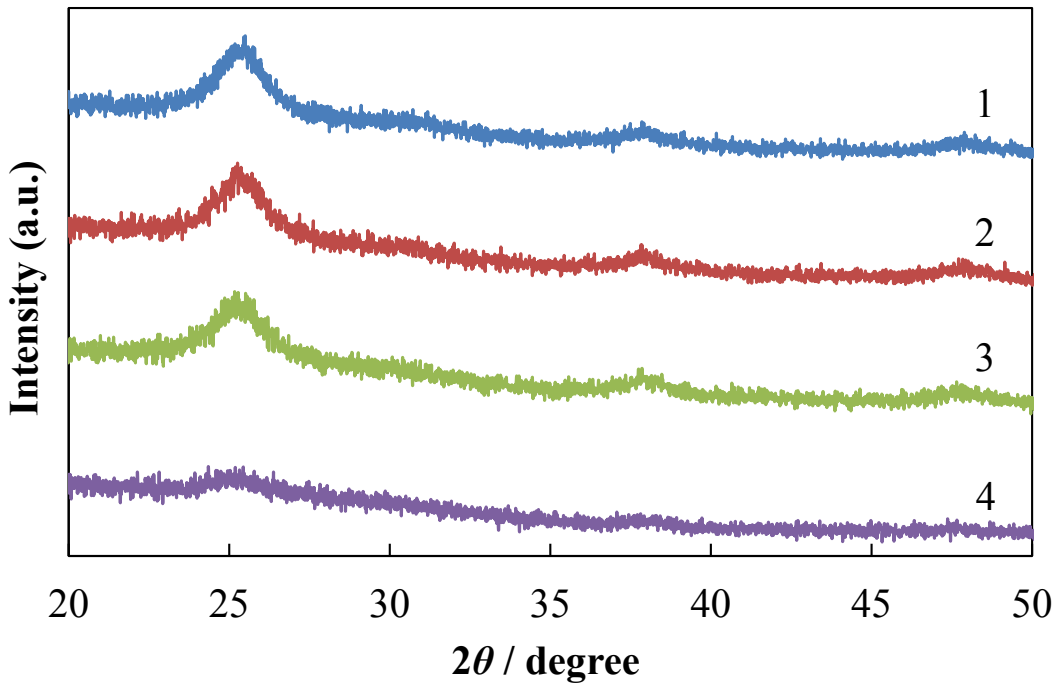

Figure 2 XRD patterns of the dye-dispersing (1) titania, (2) 0.10% allophane–titania composite, (3) 1.0% allophane–titania composite, and (4) 10% allophane–titania composite electrodes.

3.2. Photoelectric conversion properties of the electrodes

Figure 3 shows the UV-vis absorption spectra of the dye-adsorbing and dye-dispersing titania and allophane–titania composite electrodes. The amount of the dye adsorbed on the electrodes increased with an increase in the allophane content because the allophane effectively functioned as an adsorbent. The anion species exhibits absorption peaks at 460 and 485 nm (double maxima) and the dianion species exhibits a peak at 490 nm in aqueous solutions (Fujii et al., 1992). Not only the anion band, but also the dianion band was observed in all the dye-adsorbing electrodes. The amount of the dye dispersed in the electrodes also increased with the allophane content although the dye concentrations in the electrodes before the steam treatment were equal. Some dye molecules were desorbed into the water phase during the steam treatment. A higher number of the dye molecules remained in the electrodes containing a higher amount of allophane. The dye-dispersing titania and 0.1% allophane–titania electrodes exhibited peaks at around 500 nm, indicating that the dye molecules were dispersed as dianions and strongly interacted with the titania, i.e., formed the dye–titania complex (Nishikiori et al., 2011c, 2014b; Setiawan et al., 2013). The peak was shifted in the shorter wavelength direction to 490 nm with an increase in the dye concentration, indicating that the amount of the dye–titania complex decreased due to the

preferential interaction with allophane. The difference in the composition of the species between the dye-adsorbing and dye-dispersing electrodes was due to the strength of interaction with the allophane or titania and their acidity. The acidity of the hydroxyl group is expected to be higher on the allophane (silica–alumina) surface than in the titania gel (Setiawan et al., 2013).

(a)

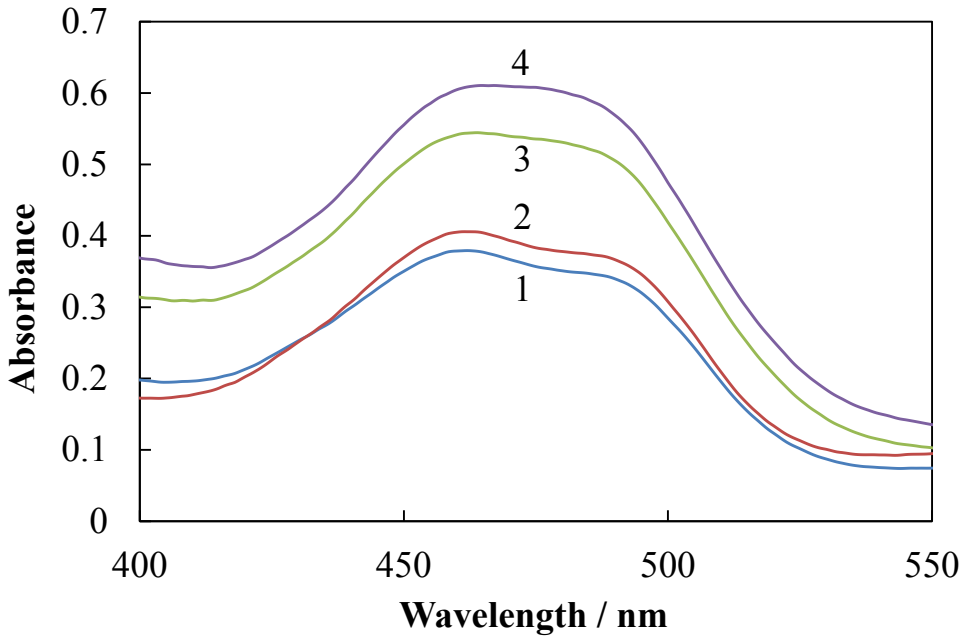

(b)

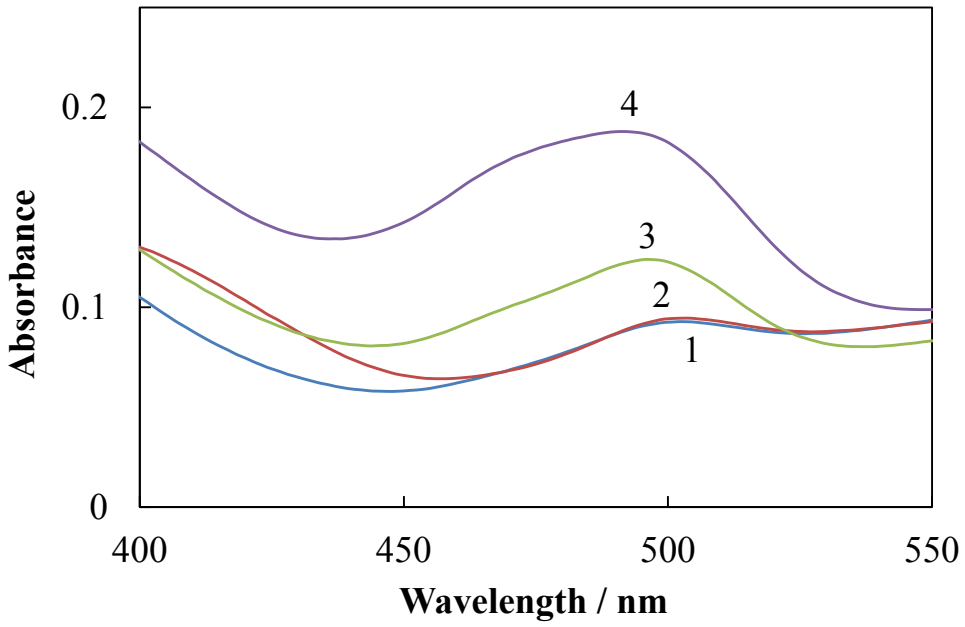

Figure 3 UV–vis absorption spectra of the (a) dye-adsorbing and (b) dye-dispersing (1) titania, (2) 0.10% allophane–titania composite, (3) 1.0% allophane–titania composite, and (4) 10% allophane–titania composite electrodes.

Figure 4 shows the photocurrent spectra of the dye-adsorbing and dye-dispersing titania and allophane–titania composite electrodes. The abscissa of the photocurrent spectra indicates the IPCE value. The IPCE values in the UV range due to the titania excitation decreased with the allophane content due to its insulating property. The shape of all the spectra in the visible range was similar to the absorption spectra of fluorescein at around 400–550 nm. This indicated that the photocurrent was generated by the injection of the excited electrons of fluorescein into the titania conduction band (Nishikiori et al., 2011c, 2014b; Setiawan et al., 2013). Strictly speaking, the IPCE values at 460 nm due to the anion species were relatively lower than those at 480–490 nm due to dianion species, which were different from the absorption spectra. This result indicated that the anion species adsorbed on the allophane surface did not efficiently inject the excited electrons into the titania conduction band due to insulating property of the allophane. There is a possibility that the allophane nanoparticles aggregated due to their high hydrophilicity and incorporated the dye molecules in the electrodes containing the higher amount of allophane. Additionally, the dye aggregation on the allophane surface can decrease the electron injection efficiency due to the energy transfer and quenching (Cid et al., 2007; Griffith et al., 2011; Kimura et al., 2012; Ozawa et al., 2011). The IPCE values of the dye-dispersing electrodes were higher than those of the dye-adsorbing electrodes due to their strong interaction between the dye and titania as previously reported (Nishikiori et al., 2011c, 2013b).

(a)

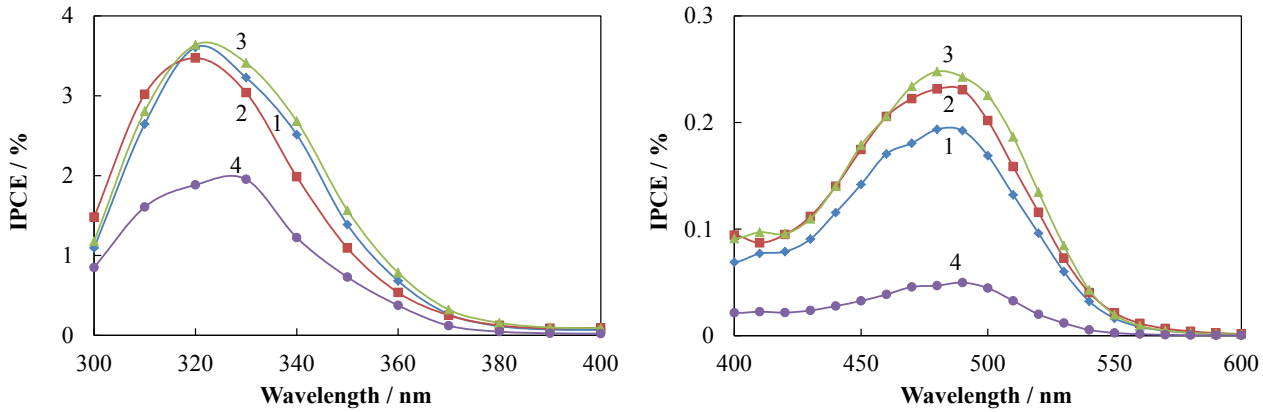

(b)

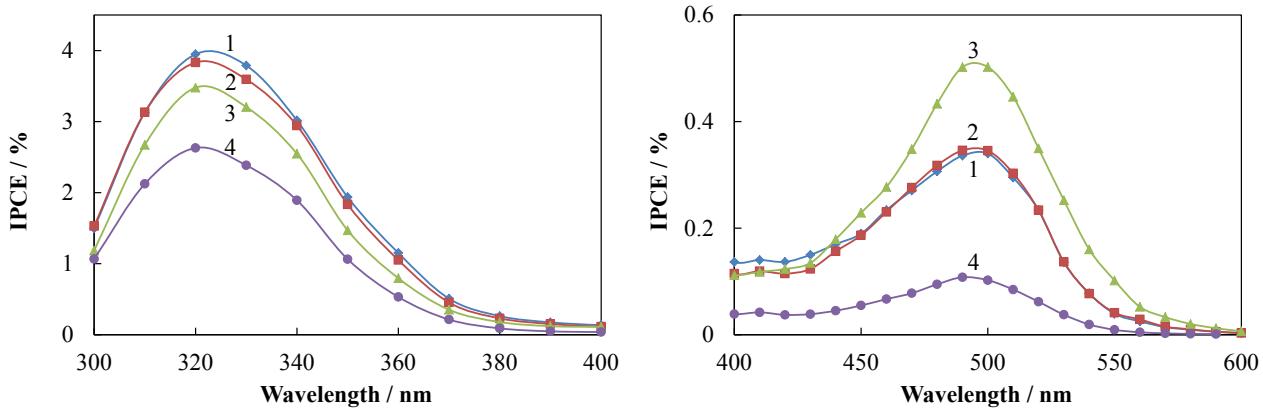

Figure 4 UV (left) and visible (right) IPCE spectra of the (a) dye-adsorbing and (b) dye-dispersing (1) titania, (2) 0.10% allophane–titania composite, (3) 1.0% allophane–titania composite, and (4) 10% allophane–titania composite electrodes.

The *J*–*V* curves of the electrode observed under the same conditions are shown in Figure 5. The short circuit current values corresponded to the IPCE values of the individual electrodes. The open circuit voltage did not significantly change with the allophane content up to 1.0%. and decreased by adding 10% allophane in both the dye-adsorbing and dye-dispersing electrodes.

This result indicated that allophane decreased the electronic conductivity of the electrode causing the back electron transfer. The photoelectric conversion efficiency was very low because the titania layer was very thin, i.e., ca. 400 nm. The APCE values in the UV and visible ranges, which originated from the excitation of the titania and the dye, respectively, were estimated in order to discuss the electron injection process from the complexes. Table 1 shows the APCE values at 350 and 490 nm and their ratios, which depended on the efficiency of the electron injection from the dye. The APCE values at 490 nm for the dye-dispersing electrodes were clearly higher than those for the dye-adsorbing electrodes. The values significantly decreased by adding 10% allophane in both electrodes. The APCE values at 350 nm were determined by the electron transport efficiency of the upper titania and titania foundation layers. The ratio of the APCE values at 350 and 490 nm for the dye-dispersing electrodes was clearly higher than that for the dye-adsorbing electrodes, indicating that the dye molecules dispersed on the surface of the individual titania nanoparticles were more effective than those adsorbed on the aggregated allophane particles.

The dye-adsorbing electrodes exhibited a very low photoelectric conversion efficiency. The present electrodes were prepared by steam treatment without heating. Their crystallite size was estimated to be 4.5–8.2 nm by the XRD analysis as shown above. The crystallite size of the samples prepared by heating at 500ºC for 30 min was 15–20 nm, which was larger than the steam-treated samples. Figures S1, S2, and S3 (Supplementary data) show the UV–vis absorption spectra, IPCE spectra, and *J–V* curves of the dye-adsorbing titania and allophane–titania

composite electrodes prepared by heating, respectively. Table S1 (Supplementary data) shows the APCE values at 350 and 490 nm for the electrodes and their ratios. All the values were improved by the heat treatment because the back electron transfer and charge recombination were effectively suppressed by increasing their crystallinities.

(a)

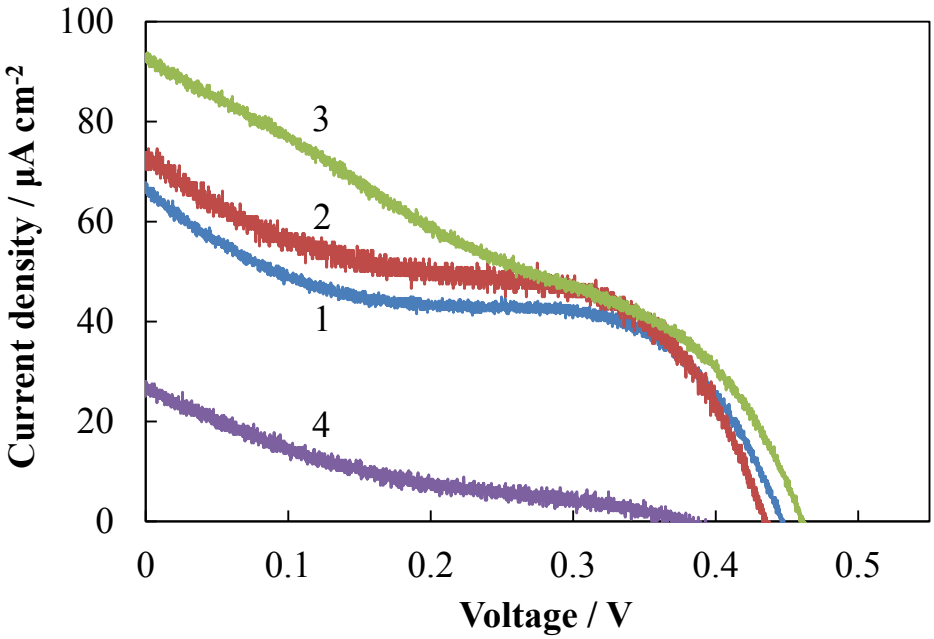

(b)

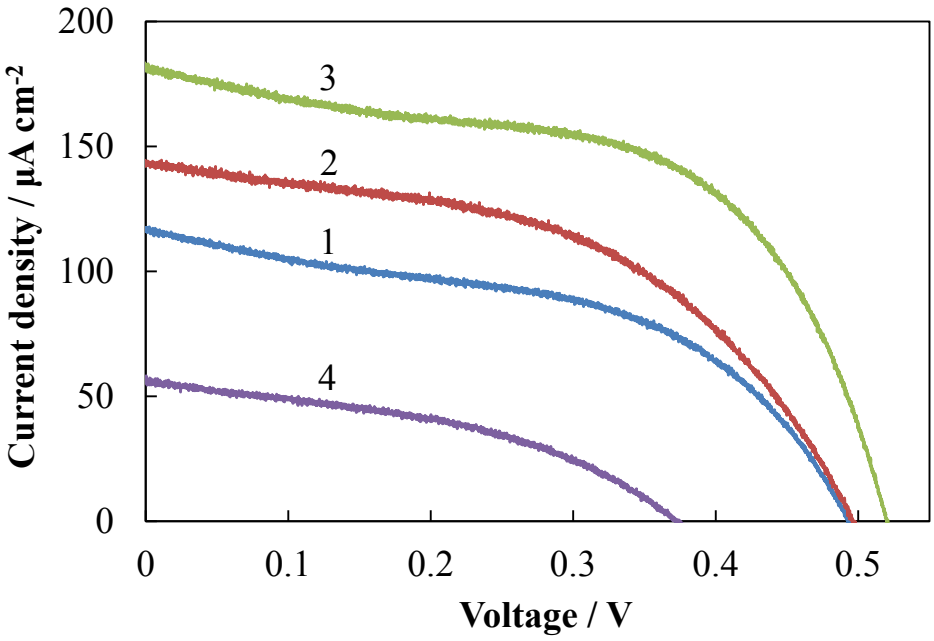

Figure 5 *J–V* curves of the (a) dye-adsorbing and (b) dye-dispersing (1) titania, (2) 0.10% allophane–titania composite, (3) 1.0% allophane–titania composite, and (4) 10% allophane–titania composite electrodes.

Table 1 APCE values at 350 and 490 nm and their ratios for the (a) dye-adsorbing and (b) dye-dispersing titania electrodes.

(a)

Electrode	APCE at 350 nm	APCE at 490 nm	Ratio
Titania	0.027	0.0038	0.14
0.1% allophane–titania	0.022	0.0044	0.20
1.0% allophane–titania	0.025	0.0040	0.16
10% allophane–titania	0.011	0.00073	0.067

(b)

Electrode	APCE at 350 nm	APCE at 490 nm	Ratio
Titania	0.042	0.030	0.71
0.1% allophane–titania	0.043	0.031	0.71
1.0% allophane–titania	0.031	0.026	0.84
10% allophane–titania	0.020	0.0042	0.21

Figure 6 shows the FTIR spectra of the dye-adsorbing and dye-dispersing 1.0% allophane–titania composite films compared to those of the dye-adsorbing allophane and the dye-adsorbing and dye-dispersing titania films. The peaks of the carboxylate COO^- antisymmetric and symmetric stretching vibrations were observed at 1597 and 1391 cm^{-1} in fluorescein, respectively. In addition,

the band at around 1490 cm^{-1} was assigned to the quinone-like C=O stretching vibration (Wang et al., 2001). The dye-adsorbing titania sample exhibited carboxylate bands at 1597 and 1389 cm^{-1} and a quinone-like band at 1479 cm^{-1}. The dye-adsorbing allophane sample exhibited carboxylate bands at around 1585 and 1387 cm^{-1} and a quinone-like band at 1456 cm^{-1}. The dye-dispersing titania sample exhibited carboxylate bands at 1574 and 1395 cm^{-1} and a quinone-like band at 1447 cm^{-1}. The significant shifts in the carboxylate and quinone-like bands are due to the interaction between the functional groups and the titanium species of titania. The peaks of the antisymmetric carboxylate and quinone-like bands were shifted to low wavenumbers by the steam treatment due to the enhancement of the interaction between the functional groups and the aluminum species of the allophane or titanium species of the titania. The order of the strong interaction between the dye and metal species was the dye-dispersing titania, dye-adsorbing allophane, and dye-adsorbing titania samples. The spectral shapes of the dye-adsorbing and dye-dispersing allophane–titania composite samples were similar to those of the dye-adsorbed allophane and dye-dispersing titania samples, respectively. This result indicated that the dye molecules strongly interact with the allophane and titania in the dye-adsorbing and dye-dispersing allophane–titania composite samples, respectively. It is suggested that the dye molecules dispersed on the titania nanoparticle surface were capped with allophane nanoparticles which prevented their desorption. The dye molecules can strongly interact with the titania in this situation. Consequently, the electron injection from

the dye to titania efficiently occurred in the dye-dispersing allophane–titania composite as shown by the photoelectrochemical measurements.

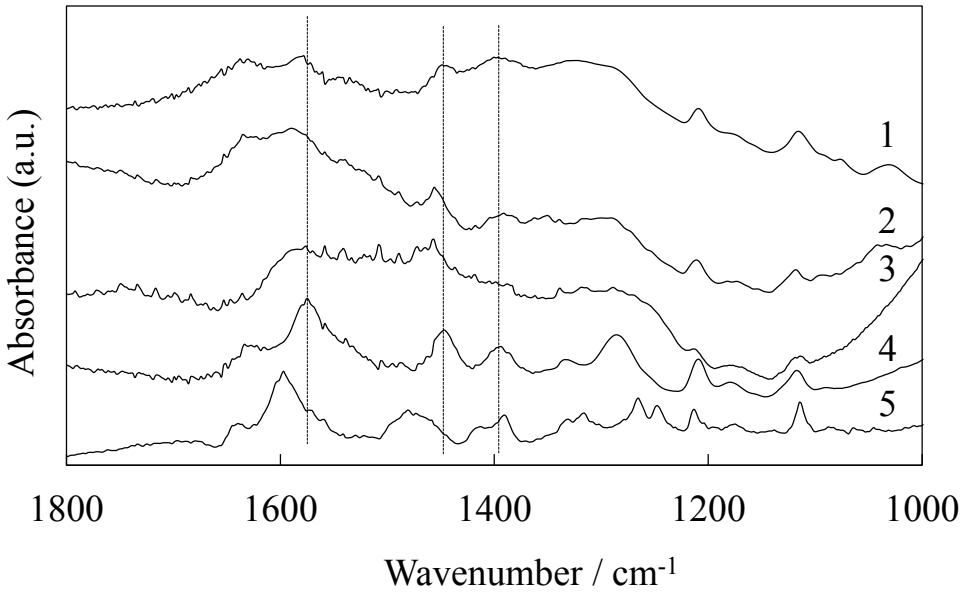

Figure 6 FTIR spectra of the (1) dye-dispersing and (2) dye-adsorbing 1.0% allophane–titania composite films, (3) dye-adsorbing allophane powder, and (4) dye-dispersing and (5) dye-adsorbing titania films.

Figure S4 (Supplementary data) shows the fluorescence spectra of the dye-adsorbing and dye-dispersing titania and allophane−titania composite electrodes. A fluorescence peak was observed at around 525 nm, mainly assigned to the anion, in the dye-adsorbing electrodes, and at around 535 nm, assigned to the dianion, in the dye-dispersing electrodes, depending on their absorption spectra (Fujii et al., 1992). The relative fluorescence quantum yields of the electrodes can be estimated from their fluorescence intensities, which were divided by their absorbance values at the excitation wavelength. The fluorescence intensities significantly increased by adding 10% allophane in both the dye-adsorbing and dye-dispersing electrodes. The intensities of the

dye-dispersing electrodes were weaker than those of the dye-adsorbing electrodes. This result indicated that some fluorescein species formed a complex with the titania surface, which were strongly quenched on the titania surface by the electron injection to the titania conduction band, especially in the dye-dispersing electrodes.

The fluorescence lifetime of the fluorescein anion and dianion was reported to be ca. 3−4 ns (Sjöback et al., 1995; Magde et al., 2002). The electron injection from the excited dye to the titania was reported to occur within 100 ps (Benkö et al., 2002; Asbury et al., 2003; Du et al., 2010). The steady state fluorescence is quenched by the electron injection (Hilgendorff and Sundström, 1998; Ramakrishna and Ghosh, 2001). This was enhanced by the dye–titania complex formation based on a previous time-resolved spectroscopic study (Setiawan et al., 2013). It was previously reported that the observed fluorescence mainly originated from the dye molecules weakly adsorbed on the titania nanoparticle surface with the lifetime of 0.22−0.41 ns (Setiawan et al., 2013).

Actually, the fluorescence decay curves of the present dye-containing titania consist of two exponential components with the lifetimes of 0.20–0.48 and 3.3–4.0 ns as shown in Figure S5 and Table S2 (Supplementary data). These values are close to those reported for the dye-adsorbing titania systems (Ramakrishna and Ghosh, 2001). The longer lifetime component is assigned to the original anion or dianion species. The shorter lifetime component can be assigned to the fluorescence of the dye interacting with the titania, which is caused by the recombination between the injected electron and the dye (Ramakrishna and Ghosh, 2001). Our previous study indicated that

the electron injection occurred within a few picoseconds and the recombination between the injected electron and the dye occurred within 20 ps (Nishikiori et al., 2007). It is reasonable that the reproduced excited-states of the dye exhibited the fluorescence with the lifetimes of 0.20–0.48 ns in the present systems. The exponential function factor for the shorter lifetime component, A_1, was much lower than that for the longer lifetime one, A_2, in the dye-adsorbing electrodes, whereas the A_1 was much higher than the A_2 in the dye-dispersing electrodes. Especially in the dye-dispersing electrodes, the dye strongly interacted with the titania and exhibited a photoinduced electron transfer to the titania. In the dye-adsorbing electrodes, the A_1 value decreased with an increase in the allophane content. In the dye-dispersing electrodes, the A_1 value slightly decreased by adding allophane. The lifetime of both the lifetime components increased by adding 10% allophane due to the enhancement of the interaction between the dye and allophane. This indicated that the dianion−titania interaction can decrease the lifetime. In this study, the enhancement of the interaction between the dye and titania increased the electron injection yield especially in the dye-dispersing electrodes with the allophane content up to 1.0%, in which the allophane nanoparticles only slightly prevented the interaction.

4. Conclusions

The fluorescein-dispersing allophane–titania composite electrodes were prepared from the titanium tetraisopropoxide sols containing the dye and allophane. The dye–titania interaction and

photoinduced electron transfer were evaluated by photoelectrochemical measurements and compared to the results of the fluorescein-adsorbing allophane–titania composite electrodes. The spectroscopic and photoelectric conversion properties of the dye-adsorbing and dye-dispersing allophane–titania composite electrodes were investigated in order to clarify the influences of the dye and allophane dispersion on the electron transfer properties. The IPCE values in the UV range decreased with an increase in the allophane content due to its insulating property in the dye-adsorbing and dye-dispersing electrodes. On the other hand, the IPCE values in the visible range decreased with an increase in the allophane content in the dye-adsorbing electrodes, whereas those were increased by adding 1.0% (Al/Ti) allophane and decreased by adding more allophane in the dye-dispersing electrodes. As a small amount of allophane nanoparticles was highly dispersed in the titania electrodes, the dye molecules were highly dispersed in the electrodes without decreasing the efficiency of the electron injection from the dye to the titania conduction band. The dye molecules dispersed on the titania nanoparticle surface were capped with allophane nanoparticles and prevented from being desorbed. The dye molecules strongly interacted with the titania nanoparticle surface and efficiently injected the excited electrons into the titania conduction band due to their high dispersion. Therefore, the dye-dispersing allophane–titania composite electrodes allowed increasing the dye content without its aggregation decreasing the electron injection efficiency.

Acknowledgment

This work was supported by JSPS KAKENHI Grant Number 24550153.

References

Antoniadou, M., Lianos, P., 2010. Production of electricity by photoelectrochemical oxidation of ethanol in a PhotoFuelCell. Appl. Catal. B 99, 307−313.

Antoniadou, M., Kondarides, D.I., Labou, D., Neophytides, S., Lianos, P., 2010. An efficient photoelectrochemical cell functioning in the presence of organic wastes. Solar Energy Mater. Solar Cells 94, 592−597.

Asbury, J.B., Anderson, N.A., Hao, E., Ai, X., Lian, T., 2003. Parameters affecting electron injection dynamics from ruthenium dyes to titanium dioxide nanocrystalline thin film. J. Phys. Chem. B 107, 7376−7386.

Benkö, G., Kallioinen, J., Korppi-Tommola, J.E.I., Yartsev, A.P., Sundström, V., 2002. Photoinduced ultrafast dye-to-semiconductor electron injection from nonthermalized and thermalized donor states. J. Am. Chem. Soc. 124, 489–493.

Bergaya, F., Theng, K.G., Lagaly, G., 2006. Handbook of Clay Science, Elsevier, Amsterdam.

Brinker, C.J., Scherer, G.W., 1990. Sol–Gel Science: The Physics and Chemistry of Sol–Gel Processing. Academic Press, San Diego.

Brinker, C.J., Frye, G.C., Hurd, A.J., Ashley, C.S., 1991a. Fundamentals of sol–gel dip coating. Thin Solid Films 201, 97–108.

Brinker, C.J., Hurd, A.J., Frye, G.C., Schunk, P.R., Ashley, C.S., 1991b. Sol–gel thin film formation. J. Ceram. Soc. Jpn. 99, 862–877.

Cameron, P.J., Peter L.M., 2003. Characterization of titanium dioxide blocking layers in dye-sensitized nanocrystalline solar cells. J. Phys. Chem. B 107, 14394−14400.

Cea, M., Seaman, J.C., Jara, A.A., Fuentes, B., Mora, M.L., Diez, M.C., 2007. Adsorption behavior of 2,4-dichlorophenol and pentachlorophenol in an allophanic soil. Chemosphere 67, 1354−1360.

Cid, J.J., Yum, J.H., Jang, S.R. Nazeeruddin, M.K. Martínez-Ferrero, E., Palomares, E., Ko, J., Grätzel, M., Torres, T., 2007. Molecular cosensitization for efficient panchromatic dye-sensitized solar cells. Angew. Chem. Int. Ed. 46, 8358−8362.

Dislich, H., 1971. New routes to multicomponent oxide glasses. Angew. Chem., Int. Ed. Engl. 10, 363–370.

Dislich, H., 1983. Glassy and crystalline systems from gels: chemical basis and technical application. J. Non-Cryst. Solids 57, 371–388.

Du, L., Furube, A., Hara, K., Katoh, R., Tachiya, M., 2010. Mechanism of particle size effect on electron injection efficiency in ruthenium dye-sensitized TiO_2 nanoparticle films. J. Phys. Chem. C 114, 8135−8143.

El Mekkawi, D., Abdel-Mottaleb, M.S.A., 2005. The interaction and photostability of some xanthenes and selected azo sensitizing dyes with TiO_2 nanoparticles. Int. J. Photoenergy 7, 95–101.

Fujii, T., Ishii, A., Takusagawa, N., Anpo, M., 1992. Fluorescence spectra and chemical species of fluorescein molecules adsorbed on a calcinated porous vycor glass. Res. Chem. Intermed. 17, 1−14.

Grätzel, M., 2003. Dye-sensitized solar cells. J. Photochem. Photobiol. C 4, 145−153.

Griffith, M.J., Mozer, A.J., Tsekouras, G., Dong, Y., Wagner, P., Wagner, K., Wallace, G.G., Mori, S., Officer, D.L., 2011. Remarkable synergistic effects in a mixed porphyrin dye-sensitized TiO_2 film. Appl. Phys. Lett. 98, 163502.

Hall, P.L., Churkman, G.J., Theng, B.K.G., 1985. Size distribution of allophane unit particles in aqueous suspensions. Clays Clay Miner. 33, 345–349.

Hanudin, E., Matsue, N., Henmi, T., 1999. Adsorption of some low molecular weight organic acids on nano-ball allophane. Clay Sci. 11, 57−72.

Hart, J.N., Menzies, D., Cheng, Y.B., Simon, G.P., Spiccia, L., 2006. TiO_2 sol–gel blocking layers for dye-sensitized solar cells. C R Chim. 9, 622−626.

Henmi, T., Wada, K., 1976. Morphology and composition of allophane. Am. Mineralogist 61, 379–390.

Hewer, T.L.R., Suárez, S. Coronado, J.M., Portela, R., Avila, P., Sanchez, B., 2009. Hybrid photocatalysts for the degradation of trichloroethylene in air. Catal. Today 143, 302−308.

Hilgendorff, M., Sundström, V., 1998. Dynamics of electron injection and recombination of dye-sensitized TiO_2 particles. J. Phys. Chem. B 102, 10505–10514.

Kaneko, M., Nemoto, J., Ueno, H., Gokan, N., Ohnuki, K., Horikawa, M., Saito, R., Shibata, T., 2006. Photoelectrochemical reaction of biomass and bio-related compounds with nanoporous TiO_2 film photoanode and O_2-reducing cathode. Electrochem. Commun. 8, 336−340.

Kimura, M., Nomoto, H., Masaki N., Mori, S., 2012. Dye molecules for simple co-sensitization process: fabrication of mixed-dye-sensitized solar cells. Angew. Chem. Int. Ed., 51, 4371−4374.

Kitagawa, Y., 1971. The "unit particle" of allophane. Am. Mineralogist 56, 465–475.

Kitayama, Y., Kodama, T., Abe, M., Shimotsuma, H., Matsuda, Y., 1998. Synthesis of titania pillared saponite in aqueous solution of acetic acid. J. Porous Mater. 5, 121−126.

Kitsui, T., Nishikiori, H., Tanaka, N., Fujii, T., 2006. Effect of steam treatment on photocurrent and dye–titania interaction in dye-doped titania gel. J. Photochem. Photobiol. A 192, 220–225.

Magde, D., Wong, R., Seybold, P.G., 2002. Fluorescence quantum yields and their relation to lifetimes of rhodamine 6G and fluorescein in nine solvents: improved absolute standards for quantum yields. Photochem. Photobiol. 75, 327–334.

Nishikiori, H., Qian, W., El-Sayed, M.A., Tanaka, N., Fujii, T., 2007. Change in titania structure from amorphousness to crystalline increasing photoinduced electron-transfer rate in dye-titania system. J. Phys. Chem. C 111, 9008−9011.

Nishikiori, H., Shindoh, J., Takahashi, N., Takagi, T., Tanaka, N., Fujii, T., 2009. Adsorption of benzene derivatives on allophane. Appl. Clay Sci. 43, 160−163.

Nishikiori, H., Kobayashi, K., Kubota, S., Tanaka, N., Fujii, T., 2010. Removal of detergents and fats from waste water using allophane. Appl. Clay Sci. 47, 325−329.

Nishikiori, H., Furukawa, M., Fujii, T., 2011a. Degradation of trichloroethylene using highly adsorptive allophane–TiO_2 nanocomposite. Appl. Catal. B 102, 470−474.

Nishikiori, H., Isomura, K., Uesugi, Y., Fujii, T., 2011b. Photofuel cells using glucose-doped titania. Appl. Catal. B 106, 250−254.

Nishikiori, H., Uesugi, Y., Takami, S., Setiawan, R.A., Fujii, T., Qian, W., El-Sayed, M.A., 2011c. Influence of steam treatment on dye–titania complex formation and photoelectric conversion property of dye-doped titania gel. J. Phys. Chem. C 115, 2880–2887.

Nishikiori, H., Kato, Y., Fujii, T., 2012a. Photocatalytic reaction on photofuel cell titania electrode. Res. Chem. Intermed. 38, 241−250.

Nishikiori, H., Ito, M., Setiawan, R.A., Kikuchi, A., Yamakami, T., Fujii, T., 2012b. Photofuel cells using allophane−titania nanocomposites. Chem. Lett. 41, 725−727.

Nishikiori, H., Uesugi, Y., Setiawan, R.A., Fujii, T., Qian, W., El-Sayed, M.A., 2012c. Photoelectric conversion properties of dye-sensitized solar cells using dye-dispersing titania. J. Phys. Chem. C 116, 4848–4854.

Nishikiori, H., Todoroki, K., Natori, D., Setiawan, R.A., Miyashita, K., Fujii, T., 2013a. Complex formation in 8-hydroxyquinoline-containing titania gel films. Chem. Lett. 42, 556–558.

Nishikiori, H., Setiawan, R.A., Miyashita, K., Teshima, K., Fujii, T., 2013b. Influence of dye dispersion on photoelectric conversion properties of dye-containing titania electrodes. Catal. Sci. Technol. 3, 1512−1519.

Nishikiori, H., Hashiguchi, S., Ito, M., Setiawan, R.A., Fujii, T., 2014a. Reaction in photofuel cells using allophane–titania nanocomposite electrodes. Appl. Catal. B 147, 246−250.

Nishikiori, H., Setiawan, R.A., Miyashita, K., Teshima, K., Fujii, T., 2014b. Influences of acid on molecular forms of fluorescein and photoinduced electron transfer in fluorescein-dispersing sol−gel titania films. Photochem. Photobiol. 90, 747−759.

Ozawa, H., Shimizu, R., Arakawa, H., 2011. Significant improvement in the conversion efficiency of black-dye-based dye-sensitized solar cells by cosensitization with organic dye. RSC Adv 2, 3198−3200.

Patrocinio, A.O.T., Paterno, L.G., Murakami Iha, N.Y., 2009. Layer-by-layer TiO_2 films as efficient blocking layers in dye-sensitized solar cells. J. Photochem. Photobiol. A 205, 23−27.

Ramakrishna, G., Ghosh, H.N., 2001. Emission from the charge transfer state of xanthene dye-sensitized TiO_2 nanoparticles: A new approach to determining back electron transfer rate and verifying the Marcus Inverted Regime. J. Phys. Chem. B 105, 7000–7008.

Setiawan, R.A., Nishikiori, H., Uesugi, Y., Miyashita, K., El-Sayed, M.A., Fujii, T., 2013. Electron transfer process in fluorescein-dispersing titania gel films observed by time-resolved fluorescence spectroscopy. J. Phys. Chem. C 117, 10308–10314.

Sharma, G.D., Balraju, P., Kumar, M., Roy, M.S., 2009. Quasi solid state dye sensitized solar cells employing a polymer electrolyte and xanthene dyes. Mater. Sci. Eng. B 162, 32–39.

Sjöback, R., Nygren, J., Kubista, M., 1995. Absorption and fluorescence properties of fluorescein. Spectrochim. Acta, A 51, L7–L21.

Suárez, S., Coronado, J.M., Portela, R., Martín, J.C., Yates, M., Avila, P., Sánchez, B., 2008. On the preparation of TiO_2−sepiolite hybrid materials for the photocatalytic degradation of TCE: influence of TiO_2 distribution in the mineralization. Environ. Sci. Technol. 42, 5892−5896.

Tao, T., Yang, J.J., Maciel, G.E., 1999. Photoinduced decomposition of trichloroethylene on soil components. Environ. Sci. Technol. 33, 74−80.

Ueno, H., Nemoto, J., Ohnuki, K., Horikawa, M., Hoshino, M., Kaneko, M., 2009. Photoelectrochemical reaction of biomass-related compounds in a biophotochemical cell comprising a nanoporous TiO_2 film photoanode and an O_2-reducing cathode. J. Appl. Electrochem. 39, 1897−1905.

van der Gaast, S.J., Wada, K., Wada, S.-I., Kakuto, Y., 1985. Small-angle X-ray powder diffraction, morphology, and structure of allophane and imogolite. Clays Clay Miner. 33, 237–243.

Wada, S., Wada, K., 1977. Density and structure of allophane. Clay Miner. 12, 289–298.

Wang, L., Roitberg, A., Meuse, C., Gaigalas, A. K., 2001. Raman and FTIR spectroscopies of fluorescein in solutions. Spectrochem. Acta, A 57, 1781−1791.

Xu, S., Lehmann, R.G., Miller, J.R., Chandra, G., 1998. Degradation of polydimethylsiloxanes (silicones) as influenced by clay minerals. Environ. Sci. Technol. 32, 1199−1206.

Yoneyama, H., Haga, S., Yamanaka, S., 1989. Photocatalytic activities of microcrystalline titania incorporated in sheet silicates of clay. J. Phys. Chem. 93, 4833−4837.

Supplementary data

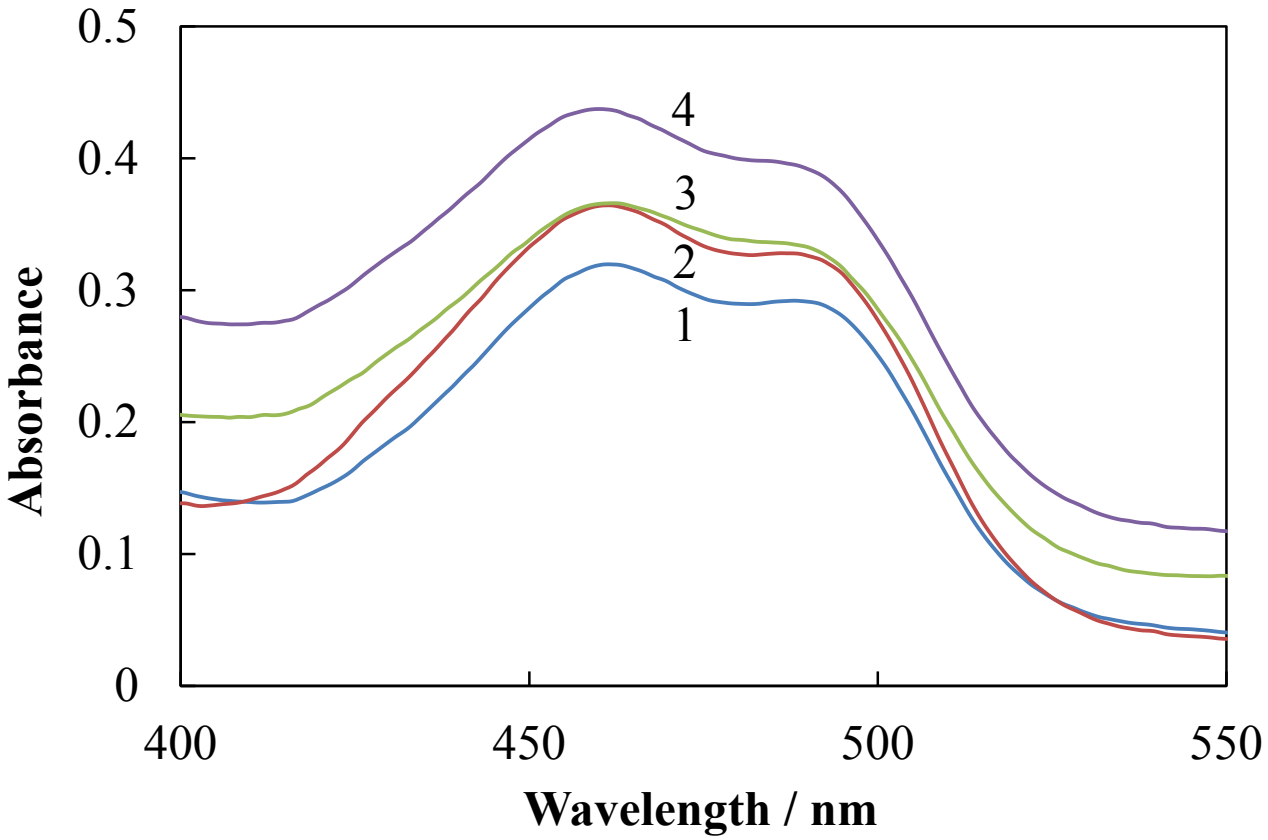

Figure S1 UV–vis absorption spectra of the dye-adsorbing (1) titania, (2) 0.10% allophane–titania composite, (3) 1.0% allophane–titania composite, and (4) 10% allophane–titania composite electrodes heated at 500ºC for 30 min.

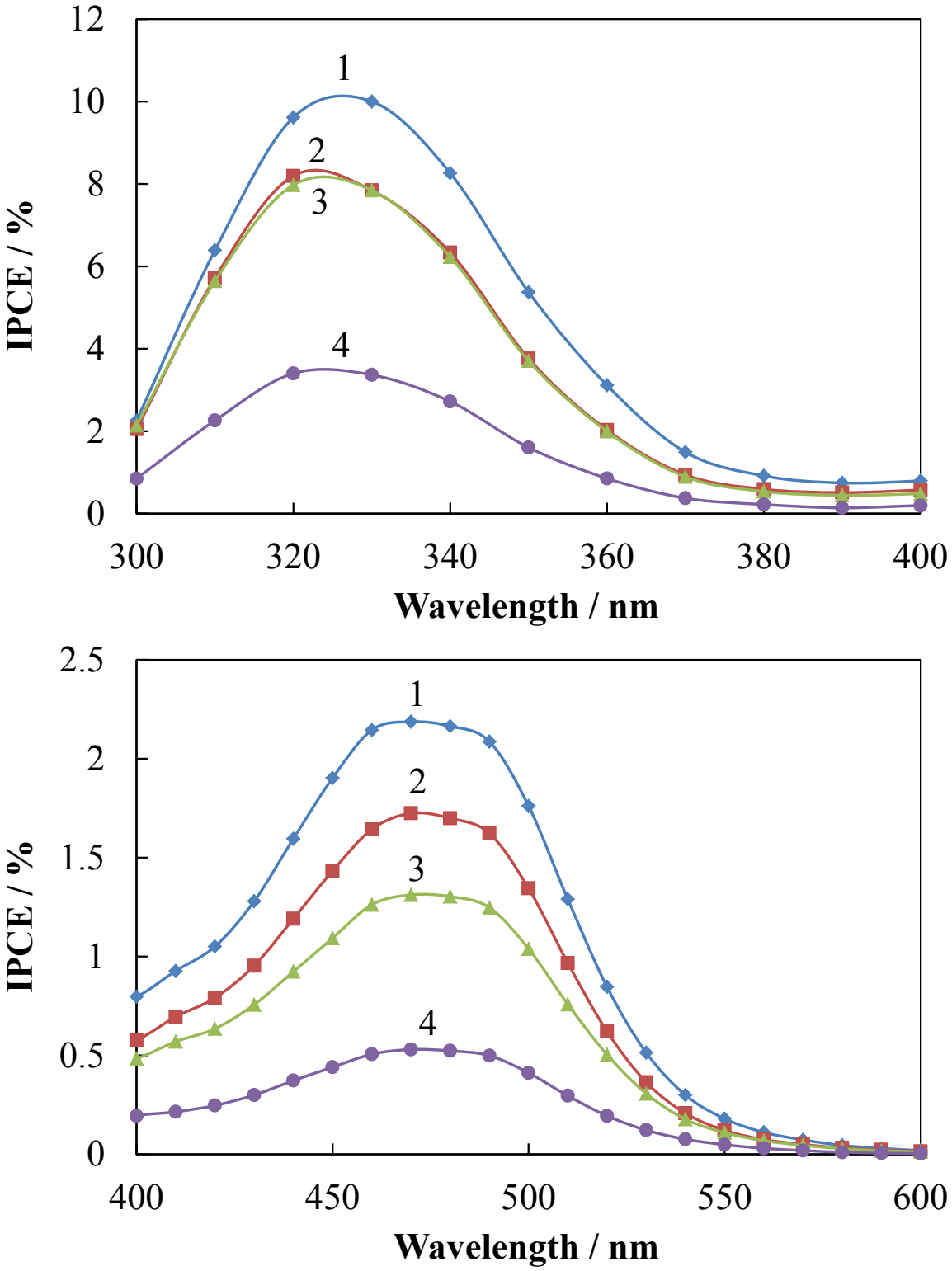

Figure S2 IPCE spectra of the dye-adsorbing (1) titania, (2) 0.10% allophane–titania composite, (3) 1.0% allophane–titania composite, and (4) 10% allophane–titania composite electrodes heated at 500ºC for 30 min.

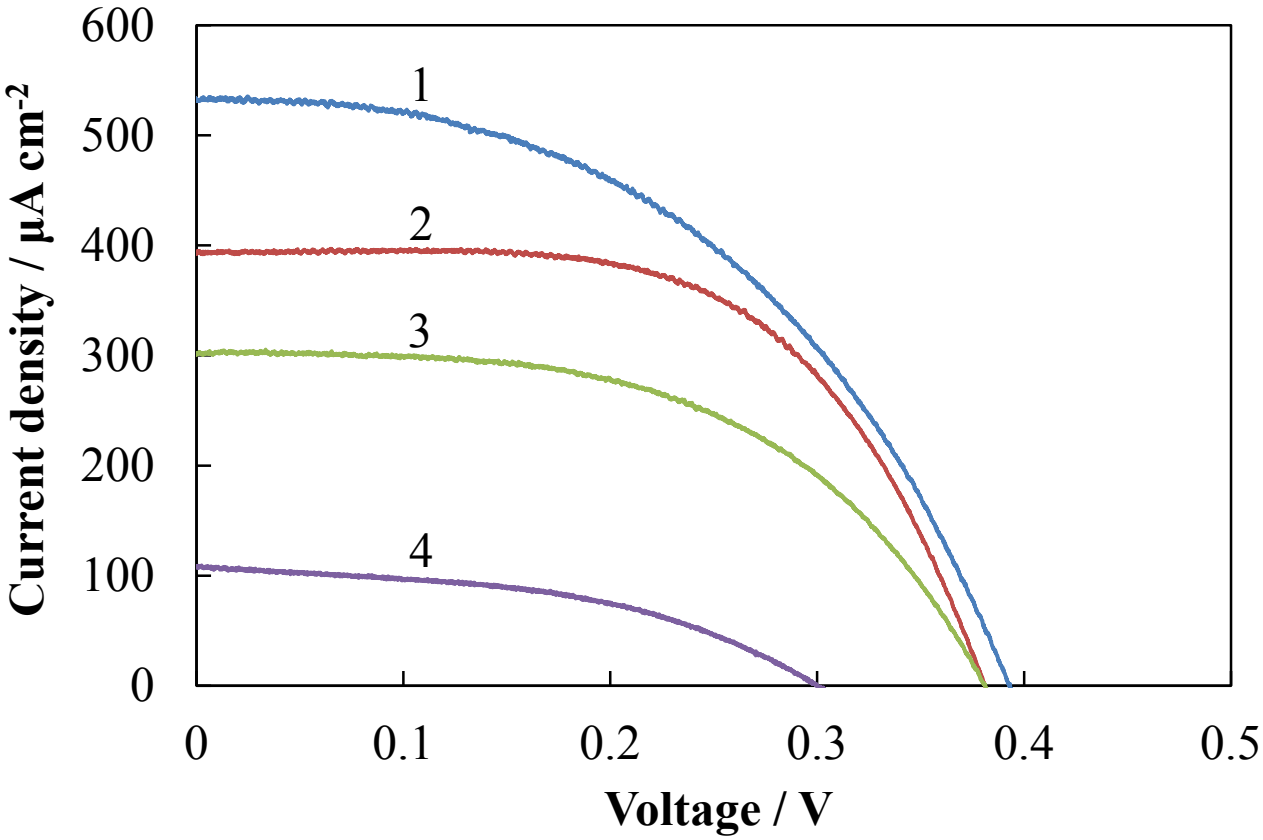

Figure S3 *J–V* curves of the dye-adsorbing (1) titania, (2) 0.10% allophane–titania composite, (3) 1.0% allophane–titania composite, and (4) 10% allophane–titania composite electrodes heated at 500ºC for 30 min.

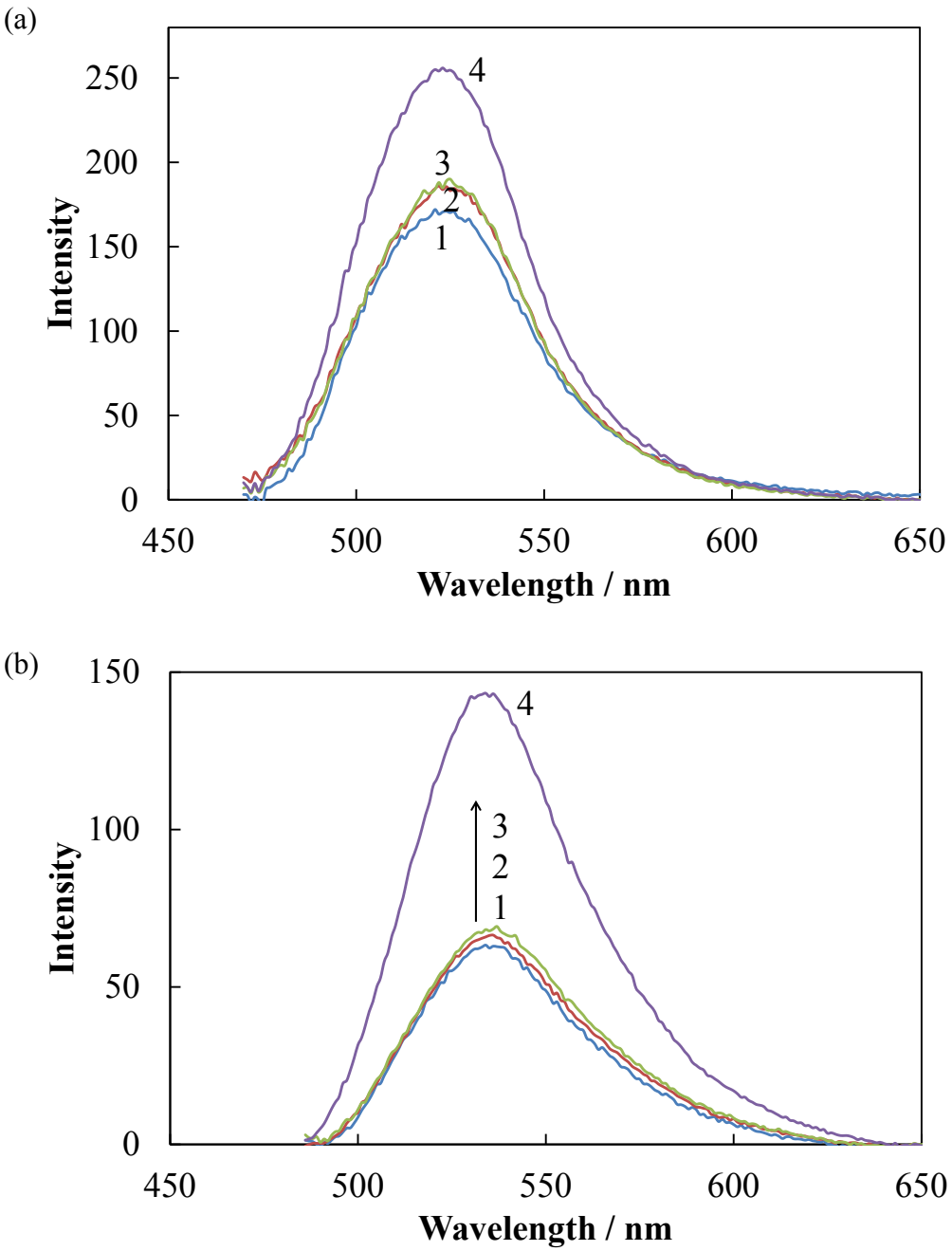

Figure S4 Fluorescence spectra of the (a) dye-adsorbing and (b) dye-dispersing (1) titania, (2) 0.10% allophane–titania composite, (3) 1.0% allophane–titania composite, and (4) 10% allophane–titania composite electrodes. The excitation wavelength was 450 nm. The fluorescence intensity was divided by the absorbance at 450 nm.

(a)

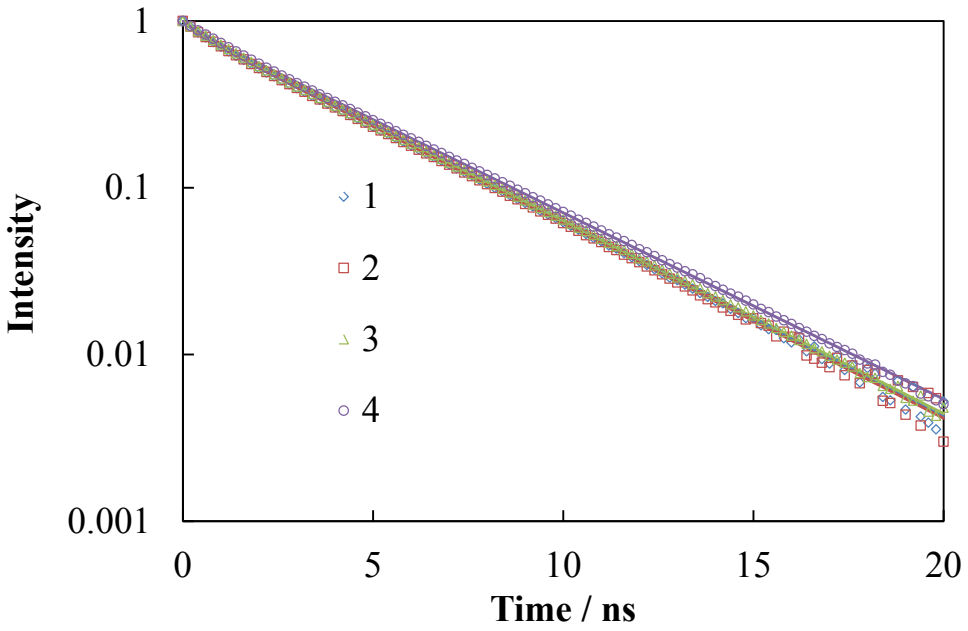

(b)

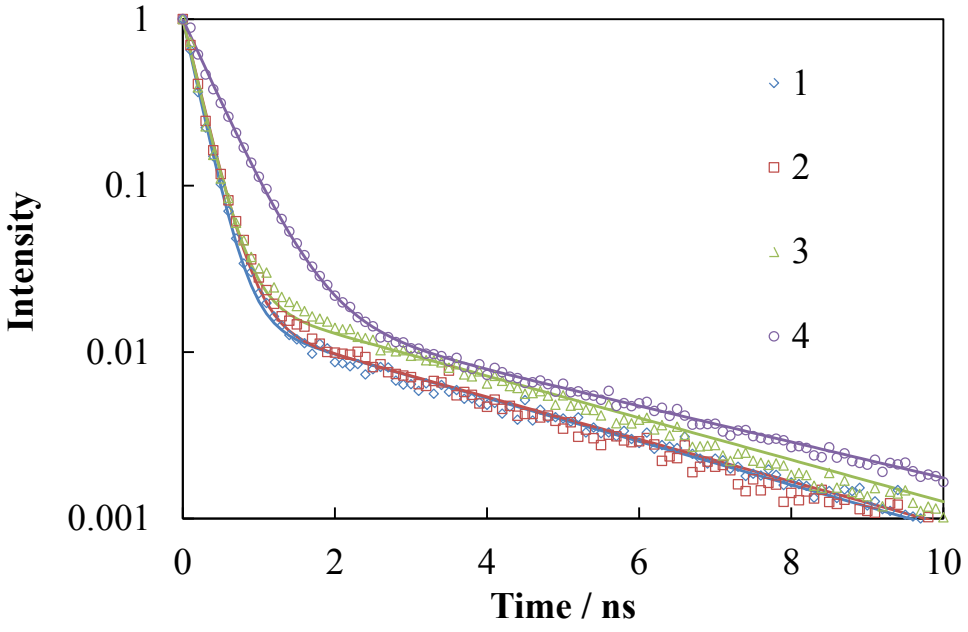

Figure S5 Fluorescence decay profiles of the (a) dye-adsorbing and (b) dye-dispersing (1) titania, (2) 0.10% allophane–titania composite, (3) 1.0% allophane–titania composite, and (4) 10% allophane–titania composite electrodes The fluorescence intensity was normalized at time 0.

A Ti:Sapphire femtosecond pulse laser and streak scope spectroscopic system were used for the time-resolved fluorescence measurements in order to obtain information about the fluorescence quenching due to the electron injection from the dye to the titania. The laser system (Clark MXR CPA 2001) generates laser pulses of 150 fs duration (FWHM) with an energy of 750 μJ at 750 nm and a repetition rate of 1 kHz. The second harmonics of the laser pulses (375 nm) was used for the excitation. The fluorescence signal was monitored using a streak scope system (Hamamatsu Photonics C4780). The fluorescence decay curves were obtained by integrating the fluorescence signals in the 500–550 nm region.

Table S1 APCE values at 350 and 490 nm and their ratios for the dye-adsorbing titania and allophane–titania composite electrodes heated at 500ºC for 30 min.

Electrode	APCE at 350 nm	APCE at 490 nm	Ratio
Titania	0.14	0.056	0.41
0.1% allophane–titania	0.097	0.039	0.40
1.0% allophane–titania	0.075	0.033	0.44
10% allophane–titania	0.025	0.012	0.50

Table S2 Fitting parameters of the time-resolved fluorescence of the (a) dye-adsorbing and (b) dye-dispersing titania and allophane–titania composite electrodes.

(a)

Electrode	τ_1 / ns	τ_2 / ns	A_1	A_2
Titania	0.452	3.75	0.113	0.887
0.1% allophane–titania	0.462	3.72	0.105	0.895
1.0% allophane–titania	0.467	3.75	0.086	0.914
10% allophane–titania	0.477	3.89	0.072	0.928

(b)

Electrode	τ_1 / ns	τ_2 / ns	A_1	A_2
Titania	0.203	3.33	0.982	0.018
0.1% allophane–titania	0.224	3.42	0.983	0.017
1.0% allophane–titania	0.218	3.45	0.977	0.023
10% allophane–titania	0.427	4.02	0.979	0.021